Cyclopropylcarbinyl-to-homoallyl carbocation equilibria influence the stereospecificity in the nucleophilic substitution of cyclopropylcarbinols

Sean P. Larmore and Pier Alexandre Champagne*

Department of Chemistry and Environmental Science, New Jersey Institute of Technology, Newark, NJ, United States

pier.a.champagne@njit.edu

ABSTRACT:
The synthesis of quaternary homoallylic halides and trichloroacetates from cyclopropylcarbinols, as reported by Marek in 2020 (*J. Am. Chem. Soc.* **2020,** *142*, 5543-5548), is one of the few reported examples of stereospecific nucleophilic substitution involving chiral bridged carbocations. However, for the phenyl-substituted substrates the stereoselectivity of the reaction is poor and a mixture of diastereomers is obtained. In order to understand the nature of the intermediates involved in this transformation and explain the loss of selectivity for certain substrates, we have performed a Density Functional Theory investigation of the reaction mechanism at the DLPNO-CCSD(T)/Def2TZVPP level of theory. Our results indicate that cyclopropylcarbinyl cations are stable intermediates in this reaction, while bicyclobutonium structures are high-energy transition structures and as such are not involved, regardless of the substitution pattern on the substrate. Instead, multiple rearrangement pathways of cyclopropylcarbinyl cations have been located, including rotations around their π-bonds and ring openings to homoallylic cations. Importantly, the relative energies of these homoallylic cations and of the activation barriers to reach them are correlated to the nature of the substituents. While direct nucleophilic attack on the chiral cyclopropylcarbinyl cation is kinetically favored for most systems, the rearrangements become competitive with nucleophilic attack for the phenyl-substituted systems, leading to a loss of selectivity through a mixture of rearranged carbocation intermediates. As such, it appears that stereospecific reactions of chiral cyclopropylcarbinyl cations depend on the ability of these cations to access homoallylic structures, from which selectivity is not guaranteed.

In 2020, Marek reported a stereospecific nucleophilic substitution of cyclopropylcarbinols **1**, forming quaternary homoallylic halides or trichloroacetates **3** (Figure 1A).[1, 2] The reaction tolerates a variety of substituents at the 1-, 3-, and 4-positions and proceeds with excellent stereocontrol with all tested nucleophiles as long as the R^3 and R^4 groups are alkyl substituents. However, for product **3b** with a phenyl group at the 4-position, epimerization at C4 is observed, the extent of which depends on the nucleophile. Experimental evidence hints at an ionization mechanism and the authors proposed a nucleophilic attack on a highly-substituted non-classical bicyclobutonium (BCB) carbocation **2** as the source of the stereoselectivity. We now report our Density Functional Theory (DFT) investigation of this reaction, which reveals that bicyclobutonium cations are high-energy structures in this system and that an unanticipated equilibrium between the cyclopropylcarbinyl (CPC) and homoallylic cations determines the stereoselectivity (or lack thereof) for this reaction.

The base cyclopropylcarbinyl/bicyclobutonium cation ($C_4H_7^+$) system has been heavily studied since Roberts' 1951 report that cyclobutyl and cyclopropylcarbinyl electrophiles solvolyse readily to form the same mixture of cyclobutyl, cyclopropylcarbinyl and homoallyl products, hinting at a common intermediate.[3] CPC/BCB cations have since been proposed as intermediates in a variety of organic reactions/rearrangements[4-12] and terpene biosynthetic pathways.[13-23] An array of spectroscopic, NMR and computational techniques have been used to probe the $C_4H_7^+$ system,[24-26] which is now understood as an equilibrating mixture of triply-degenerate σπ-bisected cyclopropylcarbinyl **I** and non-classical bicyclobutonium **II** cations (Figure 1B). These are similar in energy and interconvert stereospecifically through low-energy transition structures (TSs) on a flat potential energy surface (PES). For the $C_4H_7^+$ system, ab initio calculations at the MP2 level find that the bicyclobutonium structure **II** is more stable by about 1.8 kcal/mol.[27-29]

In contrast to $C_4H_7^+$, most substituted systems give rise to cyclopropylcarbinyl and homoallyl products rather than cyclobutyl products, which is consistent with CPC cations being the major or sole stable intermediates in those cases.[30] In fact, substituted bicyclobutonium cations are rarely stable, with the exception of simple BCB cations with silyl or alkyl groups at the 2- or 4-positions that can be lower in energy than their CPC counterparts.[29, 31-35] In some biosynthetic pathways, BCB structures that are minima on the PES have been proposed,[14, 17, 18] although always as high-energy intermediates.

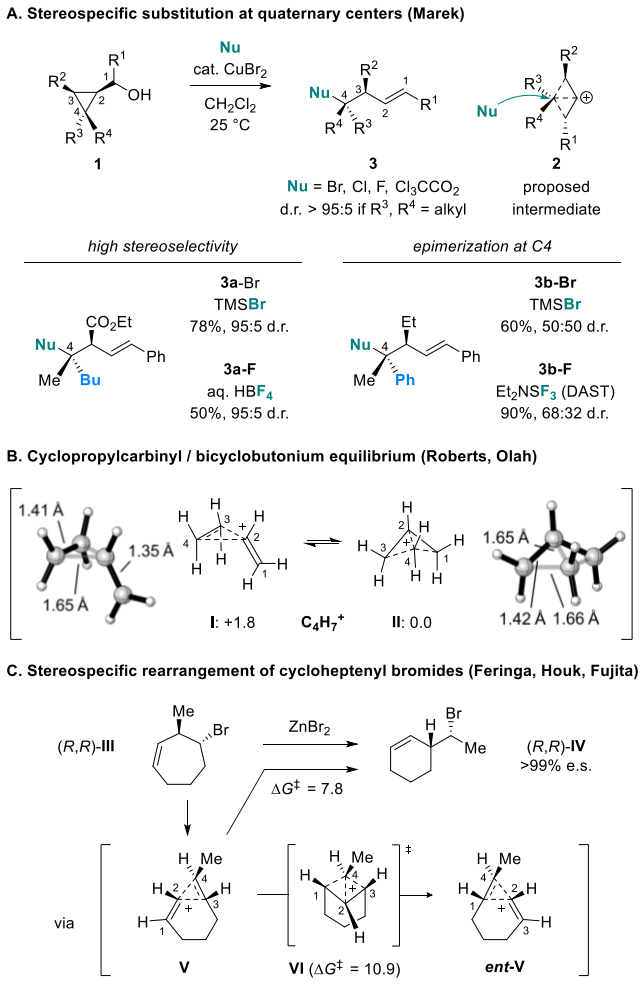

Figure 1. Free energies in kcal/mol

The stereospecific nature of CPC rearrangements implies the exciting possibility of developing stereoselective transformations involving CPC cations generated from chiral substrates. One example was reported in 2018 by Feringa, Houk and Fujita, where the Lewis acid-catalyzed rearrangement of cycloheptenyl bromide **III** proceeded with exquisite stereospecificity to the cyclohexyl derivative **IV** (Figure 1C).[36] Using DFT calculations, one of us demonstrated that in this system, the BCB cations are TSs between stable CPC intermediates, and are at least 10.9 kcal/mol higher in energy. Perhaps more importantly, we demonstrated that the CPC cation **V** formed from chiral **IV** is itself chiral, and that its bisected nature makes its racemization or rearrangement barriers larger than nucleophilic attack, leading to a stereospecific transformation.

With those precedents in mind, we set out to study the Marek reaction using DFT calculations. Hybrid DFT methods have been used successfully to study carbocationic systems[14-16, 18, 20, 35, 36] and can reproduce MP2 results for substituted CPC/BCB cations.[35] To compare the cation rearrangements to the nucleophilic attack pathways, we elected to model the fluorination reaction with BF_4^- as the nucleophile. The presence of the BF_3 Lewis acid allowed ionization mechanisms to be studied with implicit solvation without encountering charge separation issues that would be expected for a naked C-F bond ionization. For **1a**, we truncated the butyl group to an ethyl group, and the ethyl ester to a methyl ester, to simplify the conformational landscape. Four DFT methods have been tested in this system (mPW1PW91, PBE0, M06-2X, and ωB97X-D), and we found that the hybrid methods M06-2X and ωB97X-D provide better agreement with high-accuracy calculations (see Tables SI2-3). The optimization and frequency calculations of all structures were thus performed with the ωB97X-D functional, the 6-31+G(d,p) basis set and the SMD solvation model for CH_2Cl_2. Single-point energy (SPE) refinements were then obtained at the DLPNO-CCSD(T)/Def2TZVPP/SMD(CH_2Cl_2) level of theory. The final free energies presented below are obtained by combining the DLPNO-CCSD(T) SPEs with the free energy corrections obtained from the ωB97X-D geometries and frequencies. The full computational details can be found in the Supporting Information.

We first considered the nature of the cationic intermediate formed in the reaction of the model **1a**, and the fluorination products that are available from it (Figure 2). To form the cationic intermediate, we assumed that the cyclopropyl carbinol (**1a**) is first protonated by HBF_4, forming **1a·H⁺**. Loss of water with a 2.4 kcal/mol barrier leads to the first cationic intermediate **2a**, which exhibits the expected σπ-bisected geometry of a CPC cation, with two short C-C bonds (C1-C2, 1.40 Å; C3-C4, 1.47 Å) and two longer bonds (C2-C3, 1.54 Å; C2-C4, 1.64 Å). Nucleophilic attack can occur on this intermediate at any of the four carbons of the CPC core (C1-4). Attacks on C4 and C3 occur similarly to a backside S_N2 mechanism as F-C bond formation occurs simultaneously with breaking of the corresponding, elongated CPC bond, resulting in either homoallylic products **3a** or **6a** with inversion of configuration at the substituted carbon. Conversely, attacks on C1 and C2 occur similarly to nucleophilic additions on π-electrophiles, resulting in an array of cyclopropylcarbinyl and cyclobutyl regioisomers and diastereomers. Of those, only the product resulting from the most favorable TS at each position is shown in Figure 2 (others can be found in the Supporting Information). In line with the experimental results, attack on C4 has the lowest activation free energy (7.2 kcal/mol), giving rise to the observed product **3a**. Since C4 is the most substituted position and C2-C4 is the longest (weakest) bond in the structure, nucleophilic attack at C4 is preferred. Of note, the C4-epimer product **3a'** cannot be obtained directly from nucleophilic attack on **2a**, implying that some pathway must exist for this cation to epimerize.

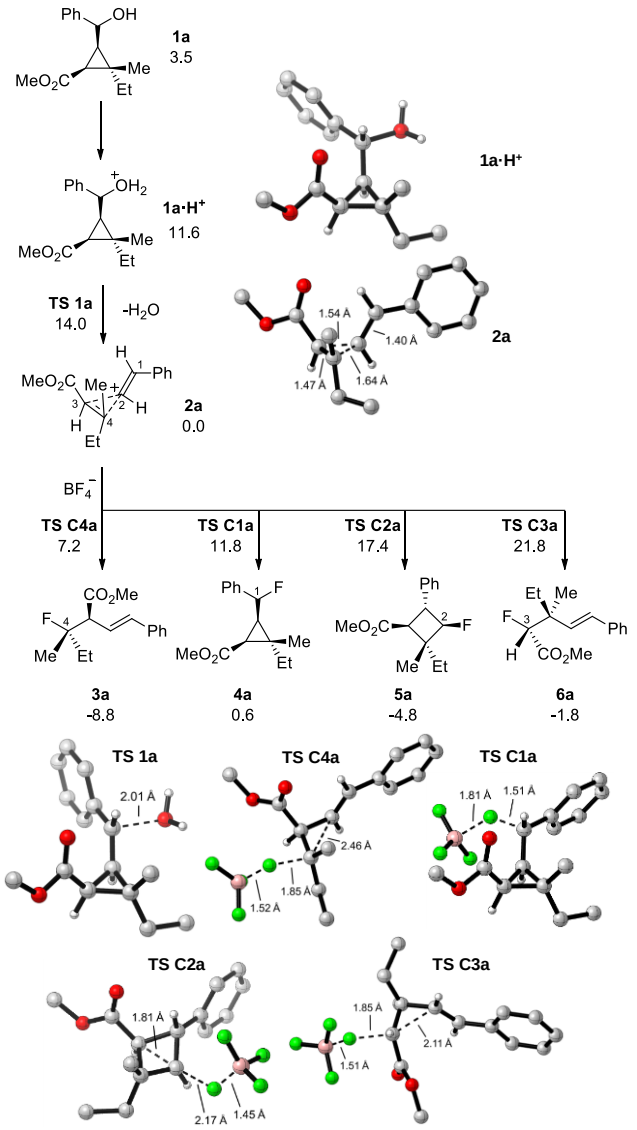

Figure 2: Ionization of **1a·H⁺** and nucleophilic attack pathways on the cationic intermediate **2a**. Free energies in kcal/mol, non-critical hydrogen atoms are hidden in the visualized structures for clarity.

The homoallylic and cyclopropylcarbinyl products **3a-6a** can be accessed directly from **2a** through nucleophilic attack. For **5a** and other cyclobutane products, we find a high energy, metastable BCB-like structure in the pathway, which is only possible in the presence of the BF_4^- counterion. Upon removal of the counter ion, this shallow minimum collapses to the CPC structure **2a** (see Figure SI3). This result hinted that the BCB cations in this system are high in energy, and we further investigated such structures to locate any stable geometries. However, all BCB structures located were in fact high-energy TSs between CPC isomers (Figure 3). Indeed, from **2a** the carbinyl carbon C1 can approach C3 (**TS 2a**, $\Delta G^{\ddagger}$ = 15.3) or C4 (**TS 5a**, $\Delta G^{\ddagger}$ = 22.2), generating new CPC-like structures **7a** and **9a**, respectively. These structures are further connected through **8a** by another set of rearrangements. Importantly, the free energy barriers to access the equilibria of Figure 3 are at least 8.1 kcal/mol higher compared to nucleophilic attack on C4 (7.2 kcal/mol for **TS C4a** vs 15.3 kcal/mol for **TS 2a**), making BCB structures unlikely to contribute to the observed reactivity. This is in line with our conclusions in the Feringa system.[36] Moreover, the large energy difference between BCB and CPC structures in **2a**, which is consistent with other substituted cyclopropylcarbinyl cations[22, 31] (including when the BCB structures are minima on the PES)[14, 17, 18], indicates that even if the ωB97X-D potential energy surface is not fully accurate and BCB structures are actually shallow minima instead of TSs, they would still be unlikely participants in the reactions of those cations.

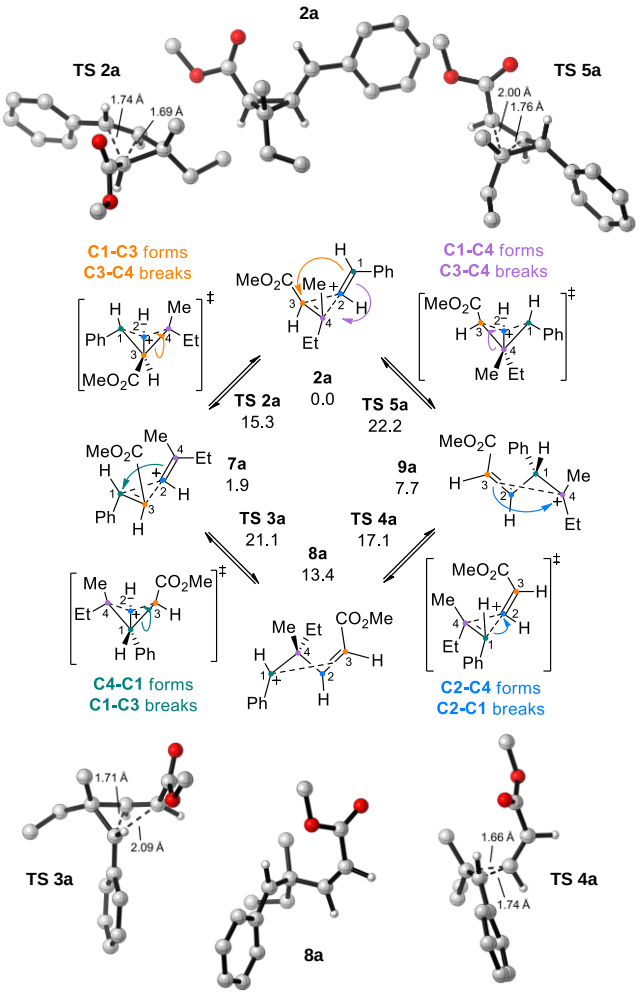

Figure 3: Bicyclobutonium pathways available to **2a**. Free energies in kcal/mol, non-critical hydrogen atoms are hidden in the visualized structures for clarity.

We then confirmed that the pathways shown in Figures 2 and 3 are similar for the phenyl-substituted substrate **1b**. Indeed, formation of the homoallyl product **3b** resulting from attack on C4 is the preferred pathway, and BCB TSs are at least 7.5 kcal/mol higher in free energy than nucleophilic attack. (Figures SI2 and SI5). As such, neither direct nucleophilic attack nor bicyclobutonium rearrangements can explain the most intriguing observation from the Marek reaction, which is the loss of diastereoselectivity for **1b** amounting to epimerization at C4. However, it can be noticed in Figure 3 that any structure placing C3 at the carbinyl position

of a CPC structure displays an "open" geometry (**8a** and **9a**), avoiding buildup of positive charge on the ester-bearing C3. This hinted at the possibility of equilibria between bisected cyclopropylcarbinyl and classical homoallylic cations in some structures.

Based on this, we wondered if the phenyl group present on C4 in **1b** allowed the CPC cation to open at the C2-C4 bond to form a homoallylic structure which could then fully epimerize. There are some precedents for such a pathway. For $C_4H_7^+$, the homoallylic structure is estimated to be 31 kcal/mol higher in energy than the CPC/BCB structures.[28] Hydroxy-substituted CPC cations adopt geometries with significant homoallylic character (with long C-C bonds).[31] The opening of CPC structures to homoallylic cations was also proposed to explain their rearrangement to allylic cations in the absence of nucleophiles.[4, 37, 38]

Finally, homoallylic cations in equilibrium with cyclopropylcarbinyl cations have been described in biosynthetic pathways, where the homoallylic structure is between 2-10 kcal/mol higher in energy than the CPC.[14, 16, 19, 21, 23]

In investigating this homoallylic cation, we discovered that C2-C4 bond opening is not the only rearrangement available to CPC cations such as **2a/b**. Indeed, a whole number of other rearrangements, which to the best of our knowledge have not been systematically considered before, are actually crucial to the selectivity of these highly substituted CPC cations (Figure 4).

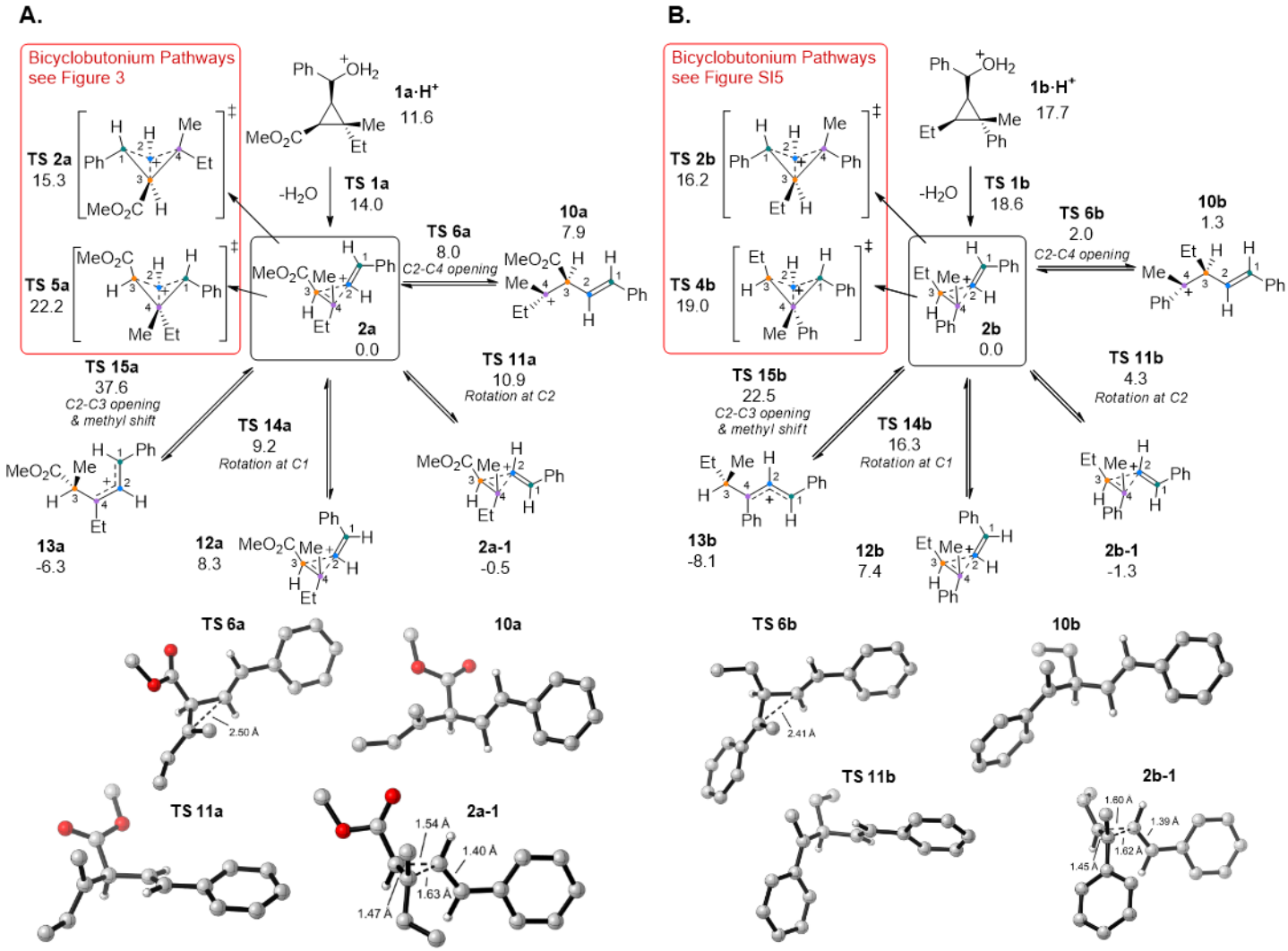

Figure 4. Rearrangement pathways available to **2a** (left) and **2b** (right). Free energies in kcal/mol, non-critical hydrogens are hidden in visualized structures for clarity.

For the C2-C4 bond opening, bond elongation happens simultaneously to the C4 carbon rotating into a planar configuration orthogonal to the C1-C2 π bond (**TS 6**), resulting in the "classical" homoallylic cationic structures **10**. **10b** is only 1.3 kcal/mol less stable than **2b** (Figure 4B), one of

the easiest CPC-to-homoallyl equilibrium reported. Of note, C4 rotation can occur in either direction, see Figure SI9**.** C2-C3 bond opening can occur similarly to C2-C4 (**TS 15b**), however since C3 only forms a secondary cation, a sequential methyl shift occurs resulting in allylic cation **13b**. This cation is more stable than any other cation on the PES, but the large activation barrier of **TS 15b** presumably prevents its formation. We also discovered that rotation around C1 or C2 is energetically accessible, forming the diastereomeric cations **12b** and **2b-1**, respectively. In C2 rotation, the CPC cation first opens to an aligned homoallyl structure (similar to **8a** and **9a**, see Figure 3), at which point the C2-C3 bond can rotate (**TS 11b**). This TS has a surprisingly small activation barrier (4.3 kcal/mol) and results in the CPC structure **2b-1**, which is more stable than **2b** by 1.3 kcal/mol. Rotation of the carbinyl carbon (C1), on the other hand, breaks the C1-C2 π bond (**TS 14b**) and as such requires 16.3 kcal/mol to form **12b**. Overall, C2-C4 opening and C2 rotation have low activation barriers , making them critical to the equilibrium, reactivity, and selectivity of **2b** (see below). We also looked into these pathways for **2a** (Figure 4A). While the rearrangements for **2a** occur with similar structures to those in **2b**, the activation barriers for these rearrangements are significantly lower for **2b** compared to **2a** (2.0 vs. 8.0 kcal/mol for C2-C4 opening and 4.3 vs. 10.9 kcal/mol for C2 rotation). This difference is most likely due to the phenyl group on C4 in **2b**, which stabilizes any variation of the homoallylic structure which is crucial to the barriers of both of these rearrangements. In comparison, **10a** is 7.9 kcal/mol higher in free energy than **2a**, and this higher energy of the homoallylic structure impacts **TS 6a** and **TS 11a**.

The fact that **2b** has various low-energy rearrangement pathways provides a plausible explanation for the difference in selectivity between **1a** and **1b**. To visualize this effect, we compared the rearrangement barriers with nucleophilic attack barriers for all available structures for both **1a** and **1b** (Figure 5). Starting from **2b** (or **2a**), three different pathways exist. First, **2b** can react immediately with a nucleophile resulting in the major product **3b** via **TS C4b**. Otherwise, **2b** is in equilibrium with a number of other rearranged structures. As discussed previously, C2-C4 opening can occur through **TS 6b** leading to **10b**. From this classical structure, nucleophilic attack can occur on both faces, resulting in either the major product **3b** or the epimer product **3b'**. Alternatively, further rotation of the C4 carbon and reformation of the C2-C4 bond (**TS 7b**) yields the epimerized CPC structure **11b**. Nucleophilic attack can occur on this structure at the C4 position resulting in **3b'**. On the other hand, C2 rotation can occur for any of these structures (**2b**, **10b**, or **11b**) resulting in analogous structures **2b-1**, **10b-1**, and **11b-1**, from which nucleophilic attack is also possible and leads to the same two diastereomeric products. The formation of the tertiary benzylic fluoride products **3b** and **3b'** is only slightly exergonic (ΔG_{rxn} = -5.4 and -5.5 kcal/mol from **2b**) and would thus appear reversible. However, we compute that the BF_3 released upon nucleophilic attack binds more strongly with water than the products (see Figure S11). As the $BF_3 \bullet H_2O$ adduct results in the hydrolysis of the BF_3 to boric and fluoroboric acids,[39] we believe that reversibility of the reaction is unlikely.

Importantly, the rearrangement barriers for **2b** are smaller than those for direct nucleophilic attack (2.0 and 4.3 vs. 7.0 kcal/mol). Thus, **2b** is in fast equilibrium with a number of low energy rearranged structures including **2b, 2b-1, 10b, 10b-1, 11b,** and **11b-1**. Nucleophilic attack can occur on each of these structures allowing formation of both **3b** and epimer **3b'**. Indeed, reaching **TS 9b-1** is as plausible as **TS C4b** or **TS C4b-1**. Thus, the energy difference between these nucleophilic attack pathways will determine the selectivity of **2b**. In this case, the two lowest-energy pathways leading to each diastereomer of the product, **TS C4b-1** and **TS 9b-1**, are similar in energy (6.9 vs. 8.1 kcal/mol, respectively), in line with the low selectivity observed in the reaction of **1b** (Figure 1A). Compared with **2b**, **2a** has less opportunities for rearrangements. In **2a**, the barriers for rearrangements are higher in energy than those for direct nucleophilic attack (8.0 and 10.9 vs. 7.2 kcal/mol), ensuring some kinetic preference for the formation of **3a**. Thus, in order to obtain **3a'**, the lowest energy pathway involves **TS 9a** (9.6 kcal/mol) through intermediate **10a**, a 2.4 kcal/mol activation free energy difference that is in line with the excellent selectivity observed for **1a**. Of note, neither **TS 8a** nor **TS 8a-1** could be located. While their energies are certainly greater than their nearest minima (7.9 and 8.3 kcal/mol respectively), we expect their energies to be roughly 2-5 kcal/mol greater that of **TS C4a** and **TS C4a-1**, by analogy with results from **2b**. Overall, our results clearly indicate that the two substrates have different potential energy surfaces, with **2a** having a larger energetic requirement for rearrangement versus nucleophilic attack, whereas **2b** rearranges faster than it engages in nucleophilic trapping, allowing the emergence of competitive pathways to form the diastereomer **3b'**.

We further analyzed the two PESs to better rationalize the different reactivity of **2a** and **2b**. From the protonated cyclopropylcarbinols **1a·H⁺/1b·H⁺**, formation of the homoallylic products **3a/b** releases a similar amount of free energy (-20.4 kcal/mol for **1a**, -23.1 for **1b**). However, the CPC cation **2b** has a greater relative stability (-17.7 from **1b·H⁺**) than cation **2a** (-11.6 from **1a·H⁺**), as **2a** is destabilized by its ester on C3 while **2b** is stabilized by its phenyl group on C4. Despite **2b** being a deeper intermediate, nucleophilic attack barriers on **2a** and **2b** are similar. However, the phenyl group on C4 of **2b** strongly stabilizes rearrangements to **10b** and **2b-1** due to the formation of a tertiary benzylic carbocation in each pathway. As such, **10b** lies 6.6 kcal/mol closer to **2b** than **10a** from **2a** (+1.3 vs +7.9 kcal/mol) and **TS 11b** lies 6.6 kcal/mol closer to **2b** than **TS 11a** from **2a** (+4.3 vs +10.9 kcal/mol). This stabilization of **2b**'s homoallylic structures significantly facilitates its rearrangements to **10b** and **2b-1**, to the point where they become kinetically preferred to nucleophilic attack. On the other hand, **2a** has significantly higher barriers to rearrangements due to its unstable homoallylic structure. As such, **2a**'s most likely pathway is direct nucleophilic trapping, forming the main product **3a**.

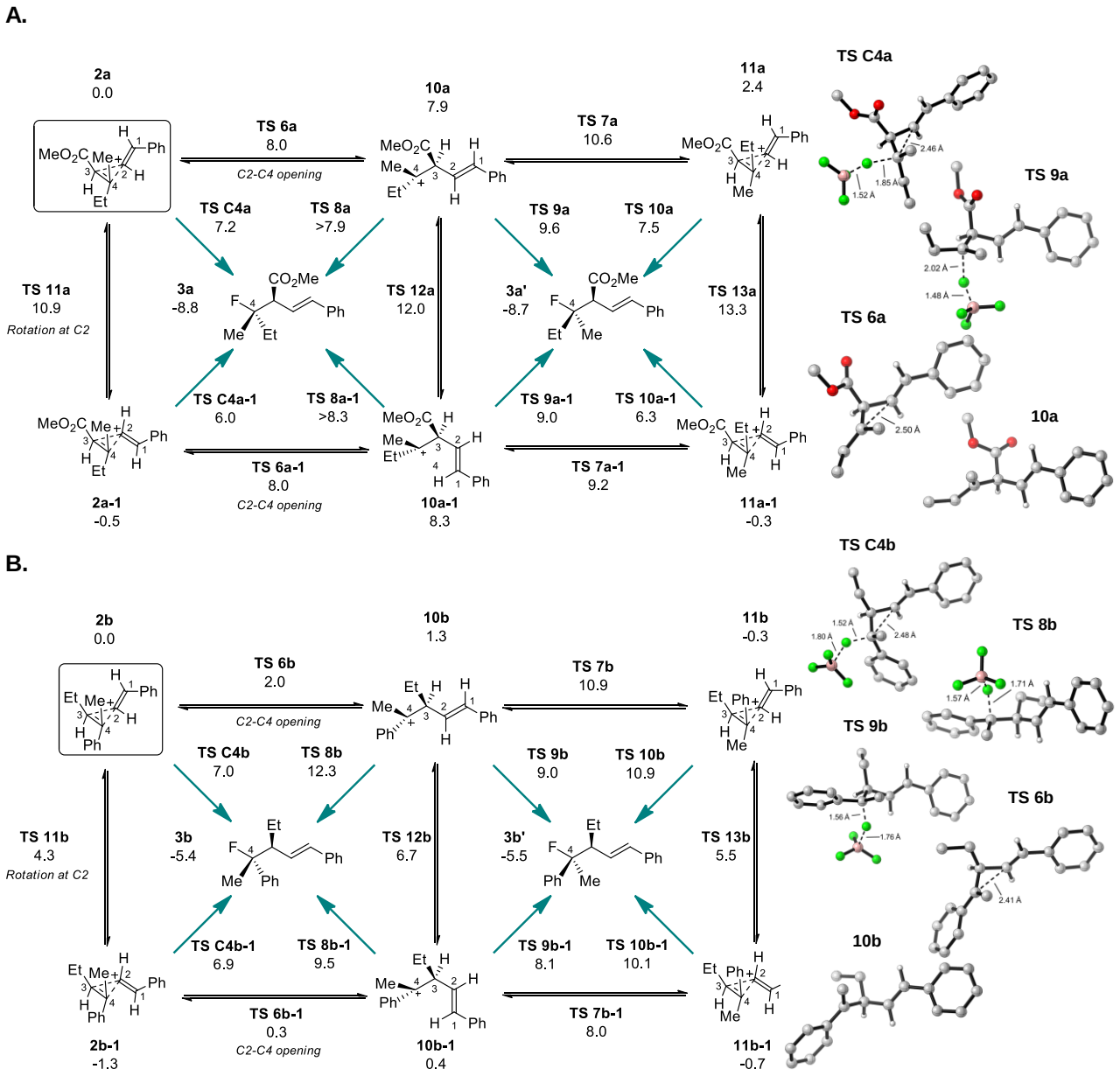

Figure 5. Nucleophilic attack and low-energy rearrangement pathways available to A) **2a** and B) **2b**. Free energies are in kcal/mol, non-critical hydrogens are hidden in visualized structures for clarity. Black equilibrium arrows depict unimolecular rearrangements, while green arrows depict nucleophilic attack by BF_4^- resulting in fluorination products and BF_3.

As the epimerization pathway is unimolecular, but the nucleophilic attack is bimolecular, different results should be expected when the identity of the nucleophile changes. For instance, for the weaker bromide nucleophile, it would be expected that the barriers for nucleophilic attack would increase while the epimerization barriers would not, leading to more epimerization when this pathway is competitive. This is what was observed for **2b** (Figure 1A). Similarly, during the preparation of this manuscript, Marek reported similar reactions involving CPC cations[40-42] and showed that phenyl-containing substrates, when reacted with highly nucleophilic trialkylaluminum compounds at lower temperatures, provide the homoallyl products without any epimerization.[40] This supports our conclusion of a CPC/homoallyl kinetic competition as the driver of the selectivity.

In conclusion, we have shown that substituted cyclopropyl carbinols generate CPC carbocations upon dehydration, and that any BCB structures are unlikely due to their high energy. These cations share the chirality of their parent substrates and have the potential to react faster with nucleophiles than they can rearrange, leading to high stereospecificity. Most importantly, we have discovered that a series of rearrangements involving CPC to homoallyl equilibria can

explain the loss of selectivity for aryl-substituted substrates. Indeed, the presence of an aryl-group on one of the cyclopropyl carbons (C3/C4) greatly increases the stability of the homoallylic cation, allowing faster rearrangements of the CPC structure relative to nucleophilic attack, leading to racemization or epimerization issues. Which substituents are required for these pathways to become competitive remains to be studied and work in this direction is underway in our group.

ASSOCIATED CONTENT

Supporting Information. Full computational details, additional figures, tables and discussions, energies and xyz coordinates of all computed structures.
Output files for all Gaussian 16 optimized geometries have been archived and can be accessed on Zenodo (DOI: 10.5281/zenodo.7569304).

AUTHOR INFORMATION

Corresponding Author

* Pier Alexandre Champagne (pier.a.champagne@njit.edu)
ORCID: 0000-0002-0546-7537

Author Contributions

The manuscript was written through contributions of all authors.

ACKNOWLEDGMENT

S.P.L. is thankful for an NJIT Provost Undergraduate Research and Innovation fellowship and a Chemical Marketing and Economics, Inc. (CME) STEM Summer Undergraduate Research fellowship, both of which helped support this work. Calculations were performed on the Lochness cluster at NJIT.

REFERENCES

1. Lanke, V.; Marek, I., Nucleophilic Substitution at Quaternary Carbon Stereocenters. *J. Am. Chem. Soc.* **2020,** *142*, 5543-5548.
2. Lanke, V.; Marek, I., Correction to "Nucleophilic Substitution at Quaternary Carbon Stereocenters". *J. Am. Chem. Soc.* **2020,** *142*, 7710-7712.
3. Roberts, J. D.; Mazur, R. H., Small-Ring Compounds. IV. Interconversion Reactions of Cyclobutyl, Cyclopropylcarbinyl and Allylcarbinyl Derivatives. *J. Am. Chem. Soc.* **1951,** *73*, 2509-2520.
4. Poulter, C. D.; Winstein, S., Solvolysis and degenerate cyclopropylcarbinyl-cyclopropylcarbinyl rearrangement of a hexamethylcyclopropylcarbinyl system. *J. Am. Chem. Soc.* **1969,** *91*, 3650-3652.
5. Geisel, M.; Grob, C. A.; Traber, R. P.; Tschudi, W., The Cyclopropylcarbinyl-Cyclobutyl-Homoallylic Rearrangement. Part III. Evidence for a symmetrical intermediate and for two discrete rearrangement processes. *Helv. Chim. Acta* **1976,** *59*, 2808-2820.
6. Friedrich, E. C.; Jassawalla, J. D. C., Methyl substituent effects upon the chemistry of 2-bicyclo[4.1.0]heptyl 3,5-dinitrobenzoates. *J. Org. Chem.* **1979,** *44*, 4224-4229.
7. Hittich, R.; Griesbaum, K., Rearrangement reactions of 1,2-dimethyl- and 1,3-dimethyl-1-cyclobutyl cations. *Tetrahedron Lett.* **1983,** *24*, 1147-1148.
8. Leeper, F. J.; Padmanabhan, P., Stereospecific nucleophilic ring-opening of a deuteriated cyclopropylcarbinol. *Tetrahedron Lett.* **1989,** *30*, 5017-5020.
9. Saunders, J.; Adamson, C.; Ganga-Sah, Y.; Lewis, A. R.; Bennet, A. J., Rearrangement and nucleophilic trapping of bicyclo [4.1. 0] hept-2-yl derived nonclassical bicyclobutenium ions. *Can. J. Chem.* **2018,** *96*, 235-240.
10. Long, P.-W.; He, T.; Oestreich, M., B(C6F5)3-Catalyzed Hydrosilylation of Vinylcyclopropanes. *Org. Lett.* **2020,** *22*, 7383-7386.
11. Dauben, W. G.; Friedrich, L. E.; Oberhaensli, P.; Aoyagi, E. I., Thujopsene rearrangements. Cyclopropylcarbinyl system. *J. Org. Chem.* **1972,** *37*, 9-13.
12. Friedrich, E. C.; Cooper, J. D., Cyclopropylcarbinyl-cyclopropylcarbinyl cation rearrangements in 2-bicyclo[n.1.0]Alkyl systems. *Tetrahedron Lett.* **1976,** *17*, 4397-4400.
13. Gutta, P.; Tantillo, D. J., Theoretical Studies on Farnesyl Cation Cyclization: Pathways to Pentalenene. *J. Am. Chem. Soc.* **2006,** *128*, 6172-6179.
14. Hong, Y. J.; Tantillo, D. J., Modes of inactivation of trichodiene synthase by a cyclopropane-containing farnesyldiphosphate analog. *Org. Biomol. Chem.* **2009,** *7*, 4101-4109.
15. Hong, Y. J.; Tantillo, D. J., How Many Secondary Carbocations Are Involved in the Biosynthesis of Avermitilol? *Org. Lett.* **2011,** *13*, 1294-1297.
16. Hong, Y. J.; Tantillo, D. J., Branching Out from the Bisabolyl Cation. Unifying Mechanistic Pathways to Barbatene, Bazzanene, Chamigrene, Chamipinene, Cumacrene, Cuprenene, Dunniene, Isobazzanene, Iso-γ-bisabolene, Isochamigrene, Laurene, Microbiotene, Sesquithujene, Sesquisabinene, Thujopsene, Trichodiene, and Widdradiene Sesquiterpenes. *J. Am. Chem. Soc.* **2014,** *136*, 2450-2463.
17. Isegawa, M.; Maeda, S.; Tantillo, D. J.; Morokuma, K., Predicting pathways for terpene formation from first principles – routes to known and new sesquiterpenes. *Chem. Sci.* **2014,** *5*, 1555-1560.
18. Hong, Y. J.; Giner, J.-L.; Tantillo, D. J., Bicyclobutonium Ions in Biosynthesis – Interconversion of Cyclopropyl-Containing Sterols from Orchids. *J. Am. Chem. Soc.* **2015,** *137*, 2085-2088.
19. Hong, Y. J.; Tantillo, D. J., The energetic viability of an unexpected skeletal rearrangement in cyclooctatin biosynthesis. *Org. Biomol. Chem.* **2015,** *13*, 10273-10278.
20. Sato, H.; Hashishin, T.; Kanazawa, J.; Miyamoto, K.; Uchiyama, M., DFT Study of a Missing Piece in Brasilane-Type Structure Biosynthesis: An

Unusual Skeletal Rearrangement. *J. Am. Chem. Soc.* **2020,** *142*, 19830-19834.
21. Sato, H.; Li, B.-X.; Takagi, T.; Wang, C.; Miyamoto, K.; Uchiyama, M., DFT Study on the Biosynthesis of Verrucosane Diterpenoids and Mangicol Sesterterpenoids: Involvement of Secondary-Carbocation-Free Reaction Cascades. *JACS Au* **2021,** *1*, 1231-1239.
22. Liang, J.; Merrill, A. T.; Laconsay, C. J.; Hou, A.; Pu, Q.; Dickschat, J. S.; Tantillo, D. J.; Wang, Q.; Peters, R. J., Deceptive Complexity in Formation of Cleistantha-8,12-diene. *Org. Lett.* **2022,** *24*, 2646-2649.
23. Sakamoto, K.; Sato, H.; Uchiyama, M., DFT Study on the Biosynthesis of Asperterpenol and Preasperterpenoid Sesterterpenoids: Exclusion of Secondary Carbocation Intermediates and Origin of Structural Diversification. *J. Org. Chem.* **2022,** *87*, 6432-6437.
24. Brown, H. C., The Cyclopropylcarbinyl Cation. In *The Nonclassical Ion Problem*, Brown, H. C., Ed. Springer US: Boston, MA, 1977; pp 69-82.
25. Olah, G. A.; Reddy, V. P.; Prakash, G. K. S., Long-lived cyclopropylcarbinyl cations. *Chem. Rev.* **1992,** *92*, 69-95.
26. Siehl, H.-U., Chapter One - The Conundrum of the (C4H7)+ Cation: Bicyclobutonium and Related Carbocations. In *Adv. Phys. Org. Chem.*, Williams, I. H.; Williams, N. H., Eds. Academic Press: 2018; Vol. 52, pp 1-47.
27. Koch, W.; Liu, B.; DeFrees, D. J., The C4H7+ cation. A theoretical investigation. *J. Am. Chem. Soc.* **1988,** *110*, 7325-7328.
28. Saunders, M.; Laidig, K. E.; Wiberg, K. B.; Schleyer, P. v. R., Structures, energies, and modes of interconversion of C4H7+ ions. *J. Am. Chem. Soc.* **1988,** *110*, 7652-7659.
29. Olah, G. A.; Surya Prakash, G. K.; Rasul, G., Ab Initio/GIAO-CCSD(T) Study of Structures, Energies, and 13C NMR Chemical Shifts of C4H7+ and C5H9+ Ions: Relative Stability and Dynamic Aspects of the Cyclopropylcarbinyl vs Bicyclobutonium Ions. *J. Am. Chem. Soc.* **2008,** *130*, 9168-9172.
30. Staral, J. S.; Yavari, I.; Roberts, J. D.; Prakash, G. K. S.; Donovan, D. J.; Olah, G. A., Low-temperature carbon-13 nuclear magnetic resonance spectroscopic investigation of C4H7+. Evidence for an equilibrium involving the nonclassical bicyclobutonium ion and the bisected cyclopropylcarbinyl cation. *J. Am. Chem. Soc.* **1978,** *100*, 8016-8018.
31. Wiberg, K. B.; Shobe, D.; Nelson, G. L., Substituent effects on cyclobutyl and cyclopropylcarbinyl cations. *J. Am. Chem. Soc.* **1993,** *115*, 10645-10652.
32. Siehl, H.-U.; Fuss, M.; Gauss, J., The 1-(Trimethylsilyl)bicyclobutonium Ion: NMR Spectroscopy, Isotope Effects, and Quantum Chemical Ab Initio Calculations of a New Hypercoordinated Carbocation. *J. Am. Chem. Soc.* **1995,** *117*, 5983-5991.
33. Creary, X.; Heffron, A.; Going, G.; Prado, M., γ-Trimethylsilylcyclobutyl Carbocation Stabilization. *J. Org. Chem.* **2015,** *80*, 1781-1788.
34. Creary, X., The cyclopropylcarbinyl route to γ-silyl carbocations. *Beilstein Journal of Organic Chemistry* **2019,** *15*, 1769-1780.
35. Creary, X., 3-t-Butyl-1-methylcyclobutyl Cation. Experimental vs Computational Insights into Tertiary Bicyclobutonium Cations. *J. Org. Chem.* **2020,** *85*, 7086-7096.
36. Goh, S. S.; Champagne, P. A.; Guduguntla, S.; Kikuchi, T.; Fujita, M.; Houk, K. N.; Feringa, B. L., Stereospecific Ring Contraction of Bromocycloheptenes through Dyotropic Rearrangements via Nonclassical Carbocation–Anion Pairs. *J. Am. Chem. Soc.* **2018,** *140*, 4986-4990.
37. Poulter, C. D.; Winstein, S., Cyclopropylcarbinyl-allyl rearrangement of a hexamethylcyclopropylcarbinyl system. *J. Am. Chem. Soc.* **1969,** *91*, 3649-3650.
38. Sorensen, T. S.; Ranganayakulu, K., Cyclopropylcarbinyl-allylcarbinyl-allyl cation rearrangements. *Tetrahedron Lett.* **1970,** *11*, 659-662.
39. Wamser, C. A., Equilibria in the System Boron Trifluoride—Water at 25°. *J. Am. Chem. Soc.* **1951,** *73*, 409-416.
40. Patel, K.; Lanke, V.; Marek, I., Stereospecific Construction of Quaternary Carbon Stereocenters from Quaternary Carbon Stereocenters. *J. Am. Chem. Soc.* **2022,** *144*, 7066-7071.
41. Chen, X.; Marek, I., Stereoinvertive Nucleophilic Substitution at Quaternary Carbon Stereocenters of Cyclopropyl Ketones and Ethers. *Angew. Chem. Int. Ed.* **2022,** *61*, e202203673.
42. Chen, X.; Patel, K.; Marek, I., Stereoselective Construction of Tertiary Homoallyl Alcohols and Ethers by Nucleophilic Substitution at Quaternary Carbon Stereocenters. *Angew. Chem. Int. Ed.* **2023,** *62*, e202212425.

For graphical abstract only: